Reactive and Functional Polymers 109 (2016) 70–78

Contents lists available at ScienceDirect

Reactive and Functional Polymers

journal homepage: www.elsevier.com/locate/react

Preparation of poly(glycolide-*co*-lactide)s through a green process: Analysis of structural, thermal, and barrier properties

Giuliana Gorrasi [a,*], Angelo Meduri [b], Paola Rizzarelli [c], Sabrina Carroccio [c], Giusy Curcuruto [c], Claudio Pellecchia [d], Daniela Pappalardo [b,e,*]

[a] Dipartimento di Ingegneria Industriale, Università di Salerno, via Giovanni Paolo II 132, 84084 Fisciano, SA, Italy
[b] Dipartimento di Scienze e Tecnologie, Università del Sannio, via dei Mulini 59/A, 82100 Benevento, Italy
[c] Istituto per i Polimeri, Compositi e Biomateriali, Consiglio Nazionale delle Ricerche, Via Paolo Gaifami, 18, 95126 Catania, Italy
[d] Dipartimento di Chimica e Biologia "Adolfo Zambelli", Università di Salerno, via Giovanni Paolo II 132, 84084 Fisciano, SA, Italy
[e] Department of Fiber and Polymer Technology, KTH, Royal Institute of Technology, Stockholm, Sweden

ARTICLE INFO

Article history:
Received 21 July 2016
Received in revised form 4 October 2016
Accepted 4 October 2016
Available online 10 October 2016

Keywords:
Ring-opening polymerization
Poly(lactide)
Poly(glycolide)
Poly(lactide-*co*-glycolide)
Barrier properties

ABSTRACT

We have successfully synthesized poly(lactide), poly(glycolide), and poly(lactide-*co*-glycolide) copolymers in bulk by ring-opening homo- and copolymerization of glycolide and L-lactide, using sodium hydride as the environmentally friendly and nontoxic initiator. Random copolymers were obtained, and the microstructure was characterized by nuclear magnetic resonance (^{1}H and ^{13}C NMR) and matrix-assisted laser desorption ionization mass spectrometry (MALDI MS). The mechanism of reaction was elucidated by analysis of the polymer end groups. Homopolymer and copolymers films and their blends were obtained, and structure and physical properties analyzed. Thermal degradation analysis showed superior characteristics of copolymers with respect to the blends. Transport properties of water vapor were also evaluated and correlated to the copolymer composition.

1. Introduction

Aliphatic polyesters such as poly(lactide) (PLA) and poly(glycolide) (PGA) are a viable degradable alternative to the petrochemical-based polymers and their diffusion is constantly increasing worldwide. Aliphatic poly(ester)s have attracted much attention because of their highly desirable sustainable development, and they are being increasingly used in all areas of everyday life. These polymers have found a broad range of practical applications from packaging for industrial products to films in agriculture [1] and represent, by far, the most used class of polymeric materials for biomedical application [2]. They can be synthesized by ring-opening polymerization (ROP) of the related cyclic esters such as lactide (LA) and glycolide (GA) by different enzymatic, cationic, anionic, or coordination-insertion polymerization mechanisms [2–3]. The most frequently used initiator is tin (II) 2-ethylhexanoate ($Sn(Oct)_2$) [2–3]. Although the Food and Drug Administration (FDA) has approved its use with a limit of 20 ppm of residual tin in commercially used medical polymers, its cytotoxicity has raised several issues [4]. Therefore, academic research is currently searching for more biologically and environmentally friendly initiators, with cost-efficient catalytic process. Several nontoxic catalysts or initiators such as magnesium, calcium, zinc, and iron complexes or enzymes have already been evaluated [2–3]. We have recently reported the polymerization of ε-caprolactone promoted by sodium hydride (NaH), both in bulk and in solution [5]. NaH was also found to be active in the ROP of other cyclic esters such as rac-β-butyrolactone [6]. It is worth noting that its use in the polymerization of cyclic diesters, such as GA and LA, has not been reported thus far. Notably, NaH is not only a commercially available, economical and easy-to-handle initiator, but it is also made on a nontoxic metal. More importantly, sodium and potassium are essential to animal and human life [7].

Copolymerization of GA and LA has been widely used to engineer the properties of PGA and PLA. Poly(glycolide-*co*-lactide)s (PLGAs) are less stiff than the parent homopolymers, and they form amorphous polymers in the composition range of 25–75%,. Copolymers with different ratios of the two monomers have been commercially developed and are being investigated for a wide range of biomedical applications [2–3, 8–10]. In detail, they have been used in medical products such as sutures, bone screws, tissue engineering scaffolds, and drug delivery systems. In this study, we describe the use of NaH as the only initiator in the ring-opening homo- and copolymerization of L-lactide and glycolide. Notably, polymerization processes have been performed in bulk, thus avoiding the utilization of solvents, and therefore adding even more value to the used process as an "environmentally friendly" method.

Here, we present the synthesis, microstructural and thermal analysis of PLGA copolymers at different compositions of LA and GA (i.e., 37% and 64% of GA). The homopolymers (PLA and PGA) were also synthesized

* Corresponding authors.
E-mail addresses: ggorrasi@unisa.it (G. Gorrasi), pappalardo@unisannio.it (D. Pappalardo).

http://dx.doi.org/10.1016/j.reactfunctpolym.2016.10.002
1381-5148/

using the same *green* experimental conditions. The obtained copolyesters and the homopolymers were characterized by nuclear magnetic resonance (NMR), size exclusion chromatography (SEC), thermogravimetric analysis (TGA) and matrix-assisted laser desorption ionization (MALDI) mass spectrometry analysis. Mechanical mixing of products with the same copolymer composition was also carried out using the synthesized pure polymers, and their thermal properties were compared. Finally, transport properties of water vapor (sorption and diffusion) and contact angle to water were evaluated and correlated to the copolymer composition.

2. Experimental section

2.1. General procedures

Moisture- and air-sensitive materials were manipulated under nitrogen using Schlenk techniques or MBraun Labmaster glovebox. Before use, glassware was dried overnight in an oven at 120 °C. Monomers (Sigma-Aldrich) were purified as follows: L-lactide was dried in vacuo with P_2O_5 for 72 h, and then stored at −30 °C in glovebox; glycolide was recrystallized from tetrahydrofuran (Delchimica, solvent distilled under N_2 over Na/benzophenone). Deuterated solvents (dimethyl sulfoxide d_6 (DMSO-d_6) and $CDCl_3$) were purchased from Euriso-top and used as received. MALDI matrices were provided by Sigma-Aldrich and used as supplied. All other reagents and solvents were commercially available and used as received.

2.2. Instruments and measurements

NMR spectra of polymers (Supporting Information S4–S9) were recorded in DMSO-d_6 at 100 °C and in $CDCl_3$ at 25 °C on a Bruker Avance 300 spectrometer (^{1}H, 300.13 MHz; ^{13}C, 75.47 MHz). The resonances are reported in parts per million (δ) and coupling constants in Hertz (J), and they are referenced to the residual solvent peak versus $Si(CH_3)_4$: DMSO-d_6 at δ 2.50 (^{1}H) and δ 39.5 (^{13}C), $CDCl_3$ at δ 7.26 (^{1}H).

SEC analyses were carried out at room temperature, in $CHCl_3$ with a Waters 515 HPLC pump, equipped with four Ultrastyragel HR columns (in the order HR4, HR3, HR2, and HR1) connected in series, and a Waters 2414 differential refractive index detector. Polymer solutions (200 μL, 5 mg/mL) were injected and eluted at a flow rate of 1 mL/min. Polymer Lab Caliber software was used to compute the average molar masses of the samples by the calibration curve obtained using a set of primary polystyrene standards.

MALDI mass spectra were recorded in reflector mode using a 4800 MALDI TOF/TOF™ Analyzer (Applied Biosystem, Framingham, MA, USA), equipped with a Nd:YAG laser (λ = 355 nm) and working in positive-ion mode. This matrix-assisted laser desorption time of flight mass spectrometry (MALDI-TOF MS) instrument is equipped with a laser having wavelength of <500 ps pulse and 200 Hz repetition rate. The laser irradiance was set slightly above threshold. For PLLA and PLGA_37 (see Table 1), trans-3-indoleacrylic acid (IAA) (10 mg/mL in THF) was selected as matrix. 2-(4-Hydroxyphenylazo)benzoic acid (HABA, 0.1 M) in 1,1,1,3,3,3-hexafluoro-2-propanol (HFIP) was used as matrix for PGA and PLGA_64 (see Table 1). Appropriate volumes of the polymer solution (5–10 mg/mL in HFIP or THF) and matrix solution were mixed to obtain ratios of 1:1, 1:2, and 1:3 (sample/matrix v/v). A small volume of 2 μL of each sample–matrix mixture was spotted on the MALDI sample holder and slowly dried to allow matrix crystallization. The resolution of the MALDI spectra reported in the text is about 10,000 (FWHM), and the mass accuracy was 5–20 ppm for masses in the range of 1000–2000 Da.

X-ray powder diffraction (*XRD*) measurements were performed using a Bruker diffractometer (equipped with a continuous scan attachment and a proportional counter) with Ni-filtered Cu Kα radiation (λ = 1.54050 Å).

TGA was performed using a Mettler TC-10 thermobalance. Dynamic measurements were performed from 30 to 800 °C at the step of 10 °C/min, under a nitrogen atmosphere or in air (flow rate 60 mL/min). Sample weights were approximately 4–5 mg. The weight loss percent and its derivate (DTG) were recorded as a function of temperature.

Differential scanning calorimetry (DSC) was performed using approximately 6 mg of samples under nitrogen flow with a TA Q100 DSC thermal analysis instrument. Three scans for each sample, in the temperature range of 50–260 °C were performed. In the initial scan, the samples were heated at 10 °C/min through fusion and left in the melt for 3 min, and cooled at 50 °C/min. Finally, a second heating at 10 °C/min was carried out. The glass transition temperatures (Tg) were calculated as the midpoint of the heat capacity change in the third scan.

Static contact angles calculated using the sessile drop method were recorded and analyzed using an OCA 15 pro contact angle meter from Data Physics Instruments GmbH with SCA20 software (version 3.4.6 build 79). Water droplets of 1 μL were gently deposited on the substrate and quickly captured by a high-resolution camera. All measurements were conducted at 35 ± 2 °C and 50 ± 5% RH. The reported contact angles are the average of at least five measurements.

Transport properties (sorption and diffusion) of water vapor were measured using the microgravimetric method through a conventional McBain spring balance system, which consists of a glass water-jacketed chamber serviced by a high-vacuum line for sample degassing and vapor removal [11]. Inside the chamber, the samples were suspended to a helical quartz spring supplied by Ruska Industries (Houston, TX, USA) having a spring constant of 1.52 cm/mg. The temperature was controlled at 35 ± 0.1 °C by a constant temperature water bath. The samples were exposed to the water vapor at fixed pressures, P. The spring position was recorded as a function of time using a cathetometer. The spring position data were converted to mass uptake data using the spring constant, and the process was followed to a constant value of

Table 1
Homo- and copolymerization of glycolide and L-lactide.[a]

Run	f_{GA}[b]	Yield [%]	F_{GA}[c]	L_{GG}[d]	L_{LL}[d]	T_{LGL}[e]	T_{GLG}[e]	M_n[f] [kDa]	Đ[f]
(1) PGA	100	19	100	–	–	–	–	/	/
(2) PLGA_64	33	57	64	1.21	0.68	1.39	1.02	/	/
(3) PLGA_37	11	39	37	1.54	2.62	0.36	2.68	10.8	1.5
(4) PLLA	0	53	–	–	–	–	–	6.1	1.4

[a] Polymerization conditions: NaH = 50 μmol, T = 140 °C, t = 180 min (90 min in the case of PGA), [monomer(s)]/[NaH] = 180.
[b] f_{GA}, molar percentage of glycolide in the feed.
[c] F_{GA}, molar percentage of glycolide in the copolymer, as determined by ^{1}H NMR.
[d] Average length of glycolidyl (GG) and lactydyl (LL) blocks in the copolymer, calculated from ^{13}C NMR (DMSO-d_6, 100 °C).
[e] Yield of the second mode of transesterification (%) of glycolidyl (LGL) and lactydyl (GLG) sequences, calculated respectively from ^{1}H NMR ($CDCl_3$, RT) and ^{13}C NMR (DMSO-d_6, 100 °C).
[f] Molar masses and dispersity assessed via SEC.

sorption for at least 24 h. By measuring the increase in weight with time, for the samples exposed to the vapor at a given partial pressure, it is possible to obtain the equilibrium value of sorbed vapor, Ceq($g_{solvent}$/100 $g_{polymer}$). Moreover, in the case of Fickian behavior, that is, a linear dependence of sorption on square root of time, it is possible to derive the mean diffusion coefficient from the linear part of the reduced sorption curve, reported as C_t/C_{eq} versus square root of time, by Eq. (1) [12]:

$$\frac{Ct}{Ceq} = \frac{4}{d}\left(\frac{Dt}{\pi}\right)^{1/2} \quad (1)$$

where C_t is the penetrant concentration at time t, C_{eq} is the equilibrium value (wt%), d is the thickness of the sample (cm), and D is the average diffusion coefficient (cm^2/s). All samples showed an ideal behavior in the investigated pressure range, which facilitated the evaluation of sorption coefficient, S, from Henry's law:

$$C_{eq} = S * p \quad (2)$$

Using Eq. (1) it was possible to derive the diffusion coefficient, D, at every fixed pressure, and the equilibrium concentration of solvent into the sample, C_{eq} (wt%). For polymer–solvent systems, the diffusion parameter is usually not constant, but depends on the vapor concentration, according to the empirical Eq. (3):

$$D = D_0\, exp(\gamma\, C_{eq}) \quad (3)$$

where D_0 (cm^2/s) is the zero concentration diffusion coefficient (related to the fractional free volume and the microstructure of the polymer)

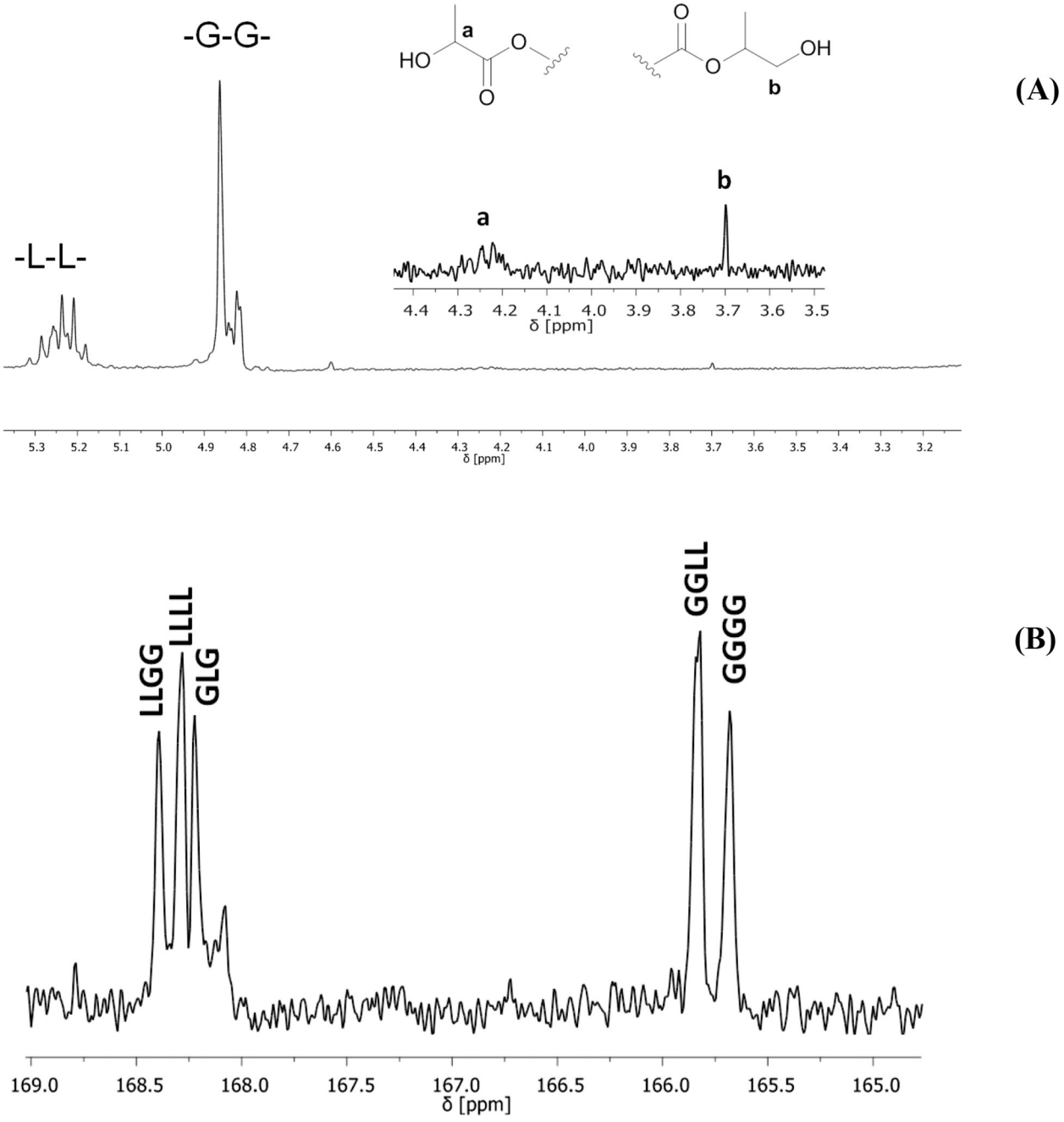

Fig. 1. (A) ^{1}H NMR (DMSO-d_6, 100 °C) spectrum of PLGA_37 (Table 1, run 3); alpha-carbonyl protons region; (B) ^{13}C NMR (DMSO-d_6, 100 °C) spectrum of PLGA_64 (Table 1, run 2); carbonyl carbons region.

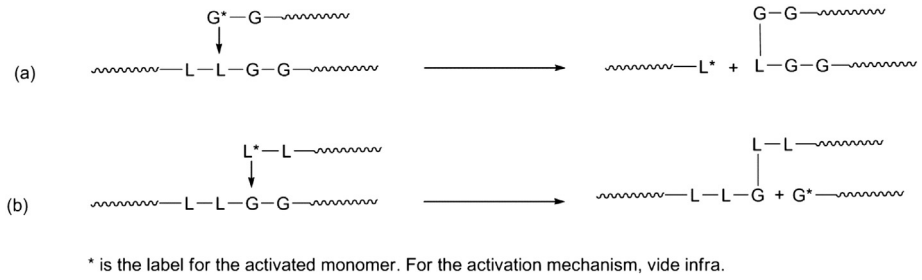

Scheme 1. Transesterification processes of the second mode for PLGA copolymers.

and γ is a coefficient that depends on the fractional free volume and the effectiveness of the penetrant to plasticize the matrix [12]. The product of sorption and diffusion gives the permeability (P):

$$P = S * D \tag{4}$$

2.3. Synthesis of the polymeric samples

In a typical polymerization run, a glass vial (20 mL) was charged with monomer(s) (total amount: 9.0 mmol) and NaH (50 μmol) in nitrogen atmosphere. The vial was placed in a silicon oil bath, preheated and thermostated at 140 °C, and magnetically stirred. After the established time (90 min for PGA and 180 min for PLA and copolymers), the vial was allowed to cool at room temperature. The reaction mixture was dissolved in wet CH_2Cl_2, and the polymer was precipitated in methanol. The precipitated polymer was recovered by filtration, washed with methanol, and dried at 60 °C in a vacuum oven.

Poly(glycolide): ^{1}H NMR (DMSO-d_6, 100 °C): 4.87 (s, 2H; $CH_2C(O)O$), 4.13 (s, 2H; CH_2OH).

Poly(L-lactide): ^{1}H NMR (DMSO-d_6, 100 °C) 5.30–5.10 (m, 1H; —$CH(CH_3)C(O)O$—), 4.23 (m, 1H; –$CH(CH_3)OH$), 3.70 (d, 2H; —$C(O)OCH(CH_3)CH_2OH$), 1.57–1.36 (m, 3H; CH_3).

^{1}H NMR ($CDCl_3$, RT) 5.36–4.91 (m, 1H; —$CH(CH_3)C(O)O$—), 4.36 (q, 1H; —$CH(CH_3)OH$), 3.78 (d, 2H; —$C(O)OCH(CH_3)CH_2OH$), 1.98–1.32 (m, 3H; CH_3).

Poly(glycolide-*co*-L-lactide): ^{1}H NMR (DMSO-d_6, 100 °C) 5.34–5.11 (m, 1H; —$CH(CH_3)C(O)O$—), 4.94–4.70 (m, 2H; —$CH_2C(O)O$—), 4.23 (m; —$OC(O)CH(CH_3)OH$), 3.70 (d, 2H; —$C(O)OCH(CH_3)CH_2OH$), 1.62–1.38 (m, 3H; CH3)·1H NMR ($CDCl_3$, RT) 5.34–5.05 (m, 1H; —$CH(CH_3)C(O)O$—), 4.93–4.55 (m, 2H; —$CH_2C(O)O$—), 4.36 (q, 1H; —$CH(CH_3)OH$), 3.78 (d, 2H; —$C(O)OCH(CH_3)CH_2OH$), 1.98–1.32 (m, 3H; CH_3).

2.4. Film preparation

Films of the synthetised samples were prepared through solvent casting technique. For samples PLLA and PLGA_37, THF was used at 40 °C, while DMSO at reflux (T ≅ 180 °C) was used for sample PLGA_64 and PGA. The solutions were cast in Petri dishes and dried in a vacuum oven for 7 days at 60 °C. Mechanical mixing was also performed using the same homopolymer compositions. Powders of the pure polymers with compositions (i) 36 wt% of PGA and 64 wt% of PLLA and (ii) 64 wt% of PGA and 36 wt% of PLLA were mixed in the dry state at room temperature in a Retsch (Germany) centrifugal ball mill (model PM 100). Sample mass were milled in a cylindrical steel jar of 12 cm^3 with three steel balls of diameter 10 mm. The rotation speed was 450 rpm and the milling time was 10 min. Films were produced in the same conditions of the PGA sample.

3. Results and discussion

3.1. Synthesis and characterization of the polymeric samples

The search and development of nontoxic initiators for the preparation of biodegradable and biocompatible aliphatic poly(esters) is a main research topic, especially when the final application for the material is a biomedical one [2–3]. While NaH was found active in the ROP of lactones (i.e., rac-β-butyrolactone and ε-caprolactone) [5–6], its use in polymerization of cyclic diesters such as GA and LA has not been reported thus far, and it represents a paramount step toward a "safe" and "harmless" polymerization method. Moreover, the homo- and copolymerization runs of GA and LA were carried out at 140 °C in bulk: notably the absence of solvents add more value to the used process as a "green" and "environmentally friendly" method. The polymerization data are summarized in Table 1. Two PLGA samples were prepared with different compositions, namely PLGA_64 and PLGA_37 with glycolide contents (FGA) of 64% and 37%, respectively. Moreover, the corresponding homopolymers PGA and PLLA were also prepared. The yield in the polymerizations never reached the full conversion, being limited to a maximum of 57% in the case of PLGA_64 (Table 1). This behavior is probably due to the high viscosity of the polymerization medium since the polymerizations were performed in bulk. The polymers were characterized by ^{1}H and ^{13}C NMR in DMSO-d_6 at 100 °C (Fig. 1(A) and (B)). The copolymer composition was evaluated by ^{1}H analysis (Fig. 1(A)). The glycolide monomer is preferentially incorporated in the polymeric chains. This feature is not surprising, because of the higher reactivity of this monomer respect to the lactide [13–14]. Because of the sensitivity of carbonyl carbons to their surroundings [15], the analysis of the ^{13}C NMR spectra in the carbonyl region (Fig. 1(B)) allows the retrieval of valuable information about the copolymer microstructure and the type of sequences. The signals were attributed to the proper sequences according to the literature. Denoting lactyl unit (—$CH(CH_3)C(=O)O$—) by "L" and glycolyl unit (—$CH_2C(=O)O$—) by "G", the analysis of the spectrum evidences the presence of not only both LLLL and GGGG homo-sequences, but also of the LLGG and GGLL hetero-sequences. This clearly indicates that glycolide and L-lactide are copolymerized and mainly random PLGA chains are formed. The average lengths of glycolidyl and lactidyl blocks (L_{GG} and L_{LL}) were calculated from the ^{13}C NMR spectra, using previously reported equations [L_{GG} = (integral of GG signal)/(integral of GL signal) + 1; L_{LL} = (integral of LL signal)/(integral of LG signal) + 1] and employing as control formula the monomer composition ratio evaluated by ^{1}H NMR ($F_{GA}/F_{LA} = L_{GG}/L_{LL}$) [16]. The values obtained for the L_{GG} and L_{LL} also indicate a highly randomized microstructure. Moreover, the presence of a signal relative to GLG sequences is also observed at 168.2 ppm in the ^{13}C spectrum. This sequence cannot be attained by simple chain propagation, and it is formed instead by transesterification of the second mode, involving the cleavage of a preformed fragment LLGG by an active G-ended polymeric chain (Scheme 1a) [17].

The amount of transesterification of the second mode relative to the sequences GLG was evaluated using the coefficients of the second mode

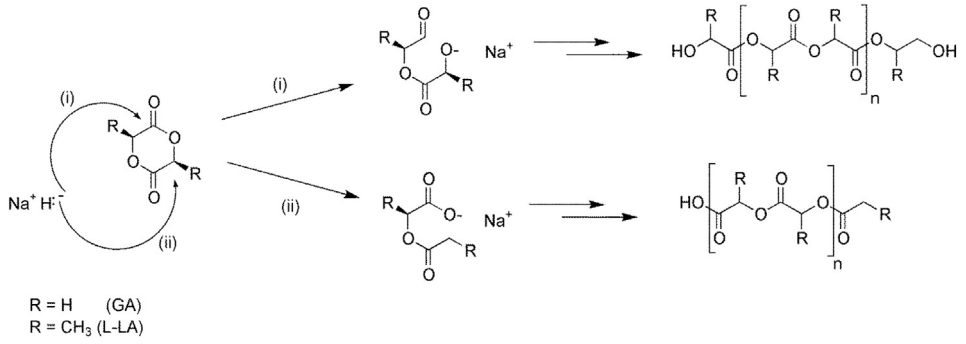

Scheme 2. Ring-opening polymerization initiated by NaH. Anionic initiation by cleavage of (i) acyl-oxygen bond and (ii) alkyl-oxygen bond.

of transesterification (T_{GLG}), as previously reported in the literature [18–19]. The other mode of transesterification, relative to the LGL sequences, can be evaluated from the signal at 4.83 ppm in the ^{1}H NMR spectrum [18]. These sequences are formed by transesterification reaction of glycolidyl segments by active lactidyl chain end (Scheme 1b) [17]. The amount of transesterification (T_{LGL}) was calculated by well-known equations [18–19]. Moreover, in the ^{1}H NMR spectra of the PLGA copolymers (Fig. 1(A)), besides the presence of the resonances attributed to the main chain, the signals at 4.23 and 3.70 ppm were detected. The quartet at 4.23 ppm can be attributed, according to the literature, to the —CH(CH_3)OH end group [17]. A broad signal at 3.70 ppm was instead attributed to the —CH(CH_3)CH_2OH end group. Notably, the same signals were also observed in the ^{1}H NMR (DMSO-d_6) spectrum of the PLLA synthesized in the presence of NaH (Table 1, run 4). The PLLA and the PLGA samples were also analyzed in $CDCl_3$ for a comparison with the literature (see Supporting Information: S1). Indeed, in the NMR spectrum of the PLLA (S1), a quartet at 4.37 ppm, characteristic of the —CH(CH_3)OH end group, and a doublet at 3.76 ppm, characteristic of the —CH(CH_3)CH_2OH end group, previously described in the literature [20], were observed. Because of the low solubility of PLGA in chloroform, the ^{1}H NMR spectrum of this sample is not well resolved, and the signals appeared quite broad. However, a multiplet at 4.36 ppm and a broad signal at 3.76 ppm were observed (S1), strongly supporting the presence of the above-described end groups, and thus confirming the data obtained in DMSO-d_6. Notably, the —CH(CH_3)CH_2OH end group can be obtained considering that the sodium hydride does not only act as initiator of the polymerization, but also as a reducing agent for the carbonyl groups (vide infra). The ROP of cyclic esters promoted by NaH obviously should proceed through an anionic mechanism. The first step of the anionic mechanism consists of the attack of the hydride anion to the cyclic diester (Scheme 2).

Two main pathways are possible: (i) H^- could attack the carbonyl carbon, leading to an acyl substitution reaction and to an aldehyde group, which may be further reduced to a primary alcohol and (ii) H^- could attack the α-carbon to the carbonyl, leading to a nucleophilic substitution and to a carboxylic end group [2]. The observation of alcohol-functionalized end groups by ^{1}H NMR supports the anionic mechanism by cleavage of acyl-oxygen bond. NaH can both initiate the polymerization and reduce the carbonyl groups. The dual role of the hydride moiety in ROP polymerization was first reported by Yasuda et al. in ε-caprolactone and δ-valerolactone polymerization using a bimetallic samarium hydride complex [21]. Analogous findings were reported for rare earth and lanthanide complexes bearing a borohydride ligand, used as initiators in the ROP of various cyclic esters [22]. Recently, we have also reported ε-caprolactone polymerization by NaH, occurring by pathway (i), as indicated by the presence of alcoholic end groups in the NMR spectra [5]. It is worth noting that mechanism (ii), i.e., the anionic initiation by cleavage of alkyl-oxygen bond could not be ruled out on the basis of the ^{1}H NMR analysis. MALDI-TOF MS has been successfully used for the structural analysis of biodegradable macromolecules,

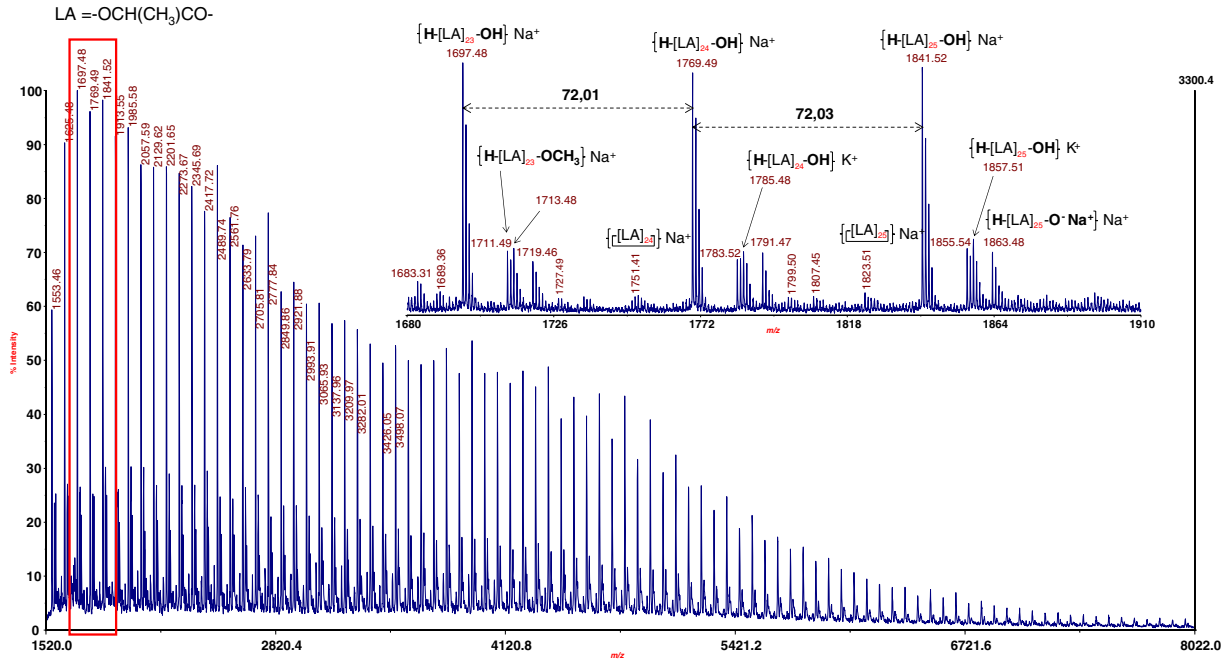

Fig. 2. MALDI mass spectrum in reflection mode of PLLA sample.

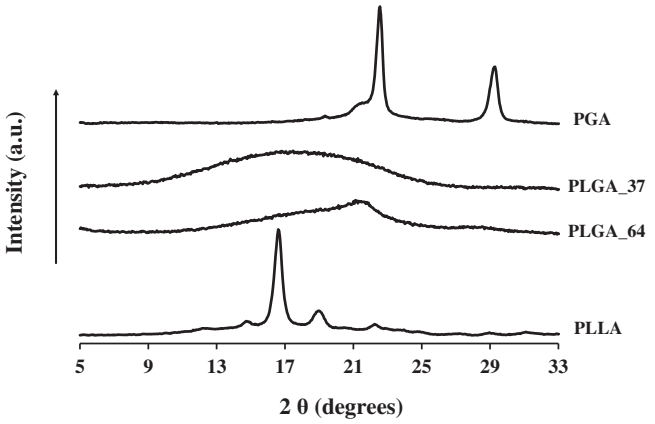

Fig. 3. XRD analysis on films of pure polymers and copolymers.

including their topology, composition, and chemical structure of the end groups [23]. Accordingly, to obtain more information about the structure of the polymer samples, MALDI analyses have been performed. Fig. 2 shows the MALDI mass spectrum, together with an enlarged portion, in reflectron mode of PLLA. The nominal mass of the repetitive unit in polylactide is 144 Da. A broadened distribution was revealed with a series of peaks spaced by 72 Da, instead of 144 Da, confirming that significant transesterification reactions occurred [22]. It extends up to *m/z* 8000 with a distribution of singly charged sodium and potassium adducts. The most abundant ions have been identified as sodium-cationized linear PLA chains, with odd and even number of repetitive units, terminated with carboxyl and hydroxyl end groups ($m/z = 1697.48 + n \times 72.02$). Less abundant ions due to cyclic species and to linear ones bearing —OH and —OCH_3 end groups were detected as well. The presence of —OCH_3 end groups could be reasonably related to the purification procedure adopted. In addition, ions at $m/z = 1683.31 \pm 72.02$ can be assigned to linear chains derived from the ROP suggested in Scheme 2. However, end groups originated from the two cleavages, (i) and (ii), have the same exact masses and cannot be discriminated by mass spectrometry. Consequently, both the mechanisms (i.e., anionic initiation by cleavage of the acyl-oxygen bond and cleavage of the alkyl-oxygen bond) are possible in the presence of NaH. Similar results were obtained for PGA and copolymer samples. In particular, mass spectra of copolymers show the presence of a large number of peaks up to *m/z* 7500. A series of ions spaced by 14 Da (the difference between 72 and 58 Da) instead of 28 Da (the difference between PLA and PGA repetitive units, respectively 144 and 116 Da) were revealed, confirming that significant transesterification reactions occurred. Again, the most abundant ions have been identified as sodium-cationized cyclic and linear PLGA chains, with odd and even number of repetitive units, terminated with carboxyl and hydroxyl end groups (see Supporting Information S2). Obviously, MALDI mass spectra of PLGA_64 and PLGA_37 show more signals because of the different compositions of cyclic and linear macromolecular chains (see Supporting Information S2).

The molar masses of the samples were determined by different approaches, such as SEC and MALDI analyses. Indeed, the determination of the molar masses of PLGA samples by SEC analyses can be quite challenging, as the radius of gyration Rg of the PLGA samples is extremely sequence and solvent dependent, thus variable with the sample composition [17]. Moreover, the assessment of the molecular weight for the PGA homopolymer (run 1, Table 1) was not possible by either SEC or NMR analysis, because the polymer is scantily soluble in almost all solvents. Analogously, sample PLGA_64, having higher amount of glycolide, is insoluble in chloroform; consequently, the determination of its molar mass by this latter technique was forbidden. It was therefore possible to carry out the SEC in $CHCl_3$ for the PLLA sample and for the PLGA_37, being poorer in glycolide (Table 1). The SEC data showed monomodal distributions with quite narrow dispersities ($Đ = 1.4 \div 1.5$). For the analysis of polymers, it has been found that the molar mass estimates provided by MALDI agree with the values obtained by conventional techniques only in the case of samples with narrow molar mass distributions. For dispersed polymer samples ($Đ > 1.2$), the MALDI results are far from the actual expected values [24], although the detection of ions at *m/z* values 1500–8000 in PLLA and PLGA_37 spectra agree well with the SEC results (Table 1).

Fig. 3 shows the X-ray analysis of the polymer and copolymer films at different chain compositions. PLLA shows the typical crystalline peaks of the α' phase located at 14.7°, 16.5°, 18.9°, and 22.2° of 2θ [25]. PGA shows two pronounced crystalline peaks at 25.5° and 29.2° of 2θ, typical of orthorhombic unit cell [26]. Both copolymers show a prevalently amorphous organization. This is an indication that the disordered macromolecular chain microstructure in both cases hinders the crystallization in either the PLLA or PGA form.

3.2. Thermal analysis

Thermal degradation of biodegradable polymers is important in understanding their usability for processing, application, and thermal recycling. TGA analysis was carried out on the films to determine the change in mass as a function of temperature increase. All samples degrade in one main step. Table 2 reports the degradation temperatures at 5%, 10%, and 50% of mass loss, in either air or nitrogen for all samples. Derived thermogravimetric (DTG) curves were then used to identify the maximum degradation temperature ($T_{deg\ max}$(°C)). Thermal degradation behavior was evaluated in either nitrogen (Fig. 4(A; B)) or air (Fig. 5(A; B)). PGA has been reported to degrade by random chain scission [27]. However, changes in degradation rates have also been observed. The polymer degrades by ester interchange processes and decarboxylation of chain ends at lower temperatures. At higher temperatures, the proportion of carbon dioxide and formaldehyde in the products formed increases, suggesting increased chain end scission [28]. The various products obtained from the pyrolysis of PGA are methyl glycolate, CO_2, formaldehydes, and ketones [29–31]. Because of the structural similarity of PLLA and PGA, PLLA degrades in a similar manner to ester interchange processes and decarboxylation from the chain ends [29,31–32]. The copolymers degrade at temperatures higher than the pure polymers, the richest in either PLLA or PGA. The copolymers

Table 2
Thermal data, evaluated from TG-DTG and DSC, for PGA, PLLA, copolymers and blends.

Sample	$T_{5\%wt\ loss}$ (nitrogen)	$T_{10\%wt\ loss}$ (nitrogen)	$T_{50\%wt\ loss}$ (nitrogen)	$T_{max\ deg}$ (nitrogen)[1]	$T_{5\%wt\ loss}$ (air)	$T_{10\%wt\ loss}$ (air)	$T_{50\%wt\ loss}$ (air)	$T_{max\ deg}$ (air)[2]	T_g
PGA	234 °C	257 °C	308 °C	318 °C	273 °C	283 °C	320 °C	328 °C	32 °C
PLLA	223 °C	260 °C	315 °C	332 °C	210 °C	230 °C	283 °C	295 °C	51 °C
PLGA_37	252 °C	295 °C	348 °C	358 °C	295 °C	313 °C	355 °C	366 °C	49 °C
PLGA_64	309 °C	319 °C	353 °C	362 °C	311 °C	323 °C	360 °C	370 °C	42 °C
$PGA37PLLA63_{mix}$	235 °C	263 °C	317 °C	330 °C	205 °C	255 °C	318 °C	333 °C	
$PGA64PLLA36_{mix}$	233 °C	260 °C	309 °C	317 °C	234 °C	263 °C	320 °C	336 °C	

[1] Evaluated from DTG (Fig. 5(B)).
[2] Evaluated from DTG (Fig. 4(B)).

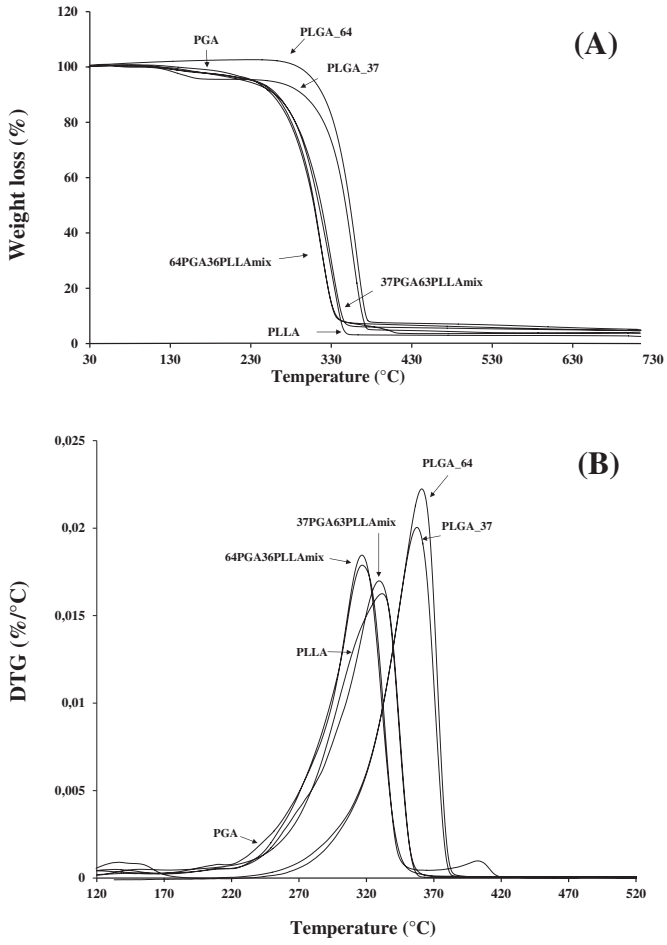

Fig. 4. TGA (A) and DTG (B) for pure polymers, copolymers, and mechanical mixtures, evaluated in nitrogen atmosphere.

show higher $T_{deg\ max}$ (°C) values in the test run in air than in nitrogen. The higher the PLLA content, the higher is the value of $T_{deg\ max}$. The degradation in air atmosphere shows a better thermal stability than in nitrogen for all samples, except for PLLA. This is in accordance with the literature, where a higher stability in oxygen atmosphere has been reported for high molecular weight PLGA, and in that case, it was ascribed to residual catalyst–oxygen interactions [33–34]. The above hypothesis can also be valid in this case, and Na–oxygen interactions can occur. Rather, it has been reported evidence for cross-linking reactions in PLGA copolymers with lower LA/GA ratios in the presence of oxygen [33–34]. Both phenomena can occur simultaneously, and might explain the observed trend. Studies are in progress to further elucidate this point. It is worth noting that both copolymers possess high degradation temperatures, in either nitrogen or air, comparable to the commercial PLLA [33]. Table 2 reports $T_{deg\ max}$ (°C) evaluated from the DTG curves for all the samples. It is evident, in either nitrogen or air, that the maximum degradation temperatures for the mechanical blends are always lower than the ones showed by the copolymers having the same homopolymer composition. Such results underline the importance of the controlled chemical synthesis, instead of the mechanical blending, for the design of materials with significantly improved physical properties.

DSC was used to evaluate the solid-state properties of copolymers, in particular the glass transition temperatures (Tg (°C)). From the calorimetric curves (Supporting Information S3), we evaluated the Tg (°C), reported in Table 2. The presence of one glass transition temperature for the copolymers confirms their homogeneous "copolymeric nature". It is evident that the Tg (°C) is a function of the prevalent component.

3.3. Transport properties of water vapor

Microbial assimilation of bio-polymers is generally preceded by enzymatic or nonenzymatic hydrolysis; therefore, the analysis of the solubility and diffusion of water molecules is of fundamental importance to reveal whether the hydrolysis process is controlled by reaction or diffusion [35]. Chain microstructure could influence the transport phenomena of small molecules through a polymeric matrix from either a thermodynamic or kinetic viewpoint. For this purpose, the thermodynamic parameter, sorption (S), the kinetic parameter, diffusion (D), and their product, permeability ($P = S*D$), for the synthesized homopolymers and copolymers were analyzed. Fig. 6(A) shows the sorption isotherms of the homopolymers and copolymers as C_{eq} (wt%) of water vapor as a function of pressure (atm). According to the literature, PGA is more hydrophilic than PLLA [33], the copolymers show intermediate values of C_{eq} (wt%) of water in the investigated pressure range. Table 3 reports the sorption data, evaluated according to Eq. (2). Fig. 6(B) shows the diffusion coefficients of all samples, as a function of C_{eq} (wt%). According to the literature, PGA shows a lower diffusion of PLLA with respect to water vapor [33]. We extrapolated the thermodynamic diffusion coefficient, D_0 (cm^2/s), according to Eq. (3). The permeability, as product of sorption and diffusion, was then evaluated for all the samples. Data are reported in Table 3. It has been shown that the degree of crystallinity does not significantly affect the diffusion parameter of PLLA [36–37]. We extrapolated from data in ref. 33 that the value of D_0 (cm^2/s) at 36.5 °C is very close to the one at the temperature of our experiments (i.e., 35 °C), that is, 6.98×10^{-8} cm^2/s.

For PGA, the degree of crystallinity significantly affects the diffusion [36]. We then also extrapolated [33] the D_0 (cm^2/s) for amorphous PGA, that is, 1.09×10^{-10} cm^2/s, about one order of magnitude lower than the value obtained in this study and in ref. 33 for crystalline PGA. The

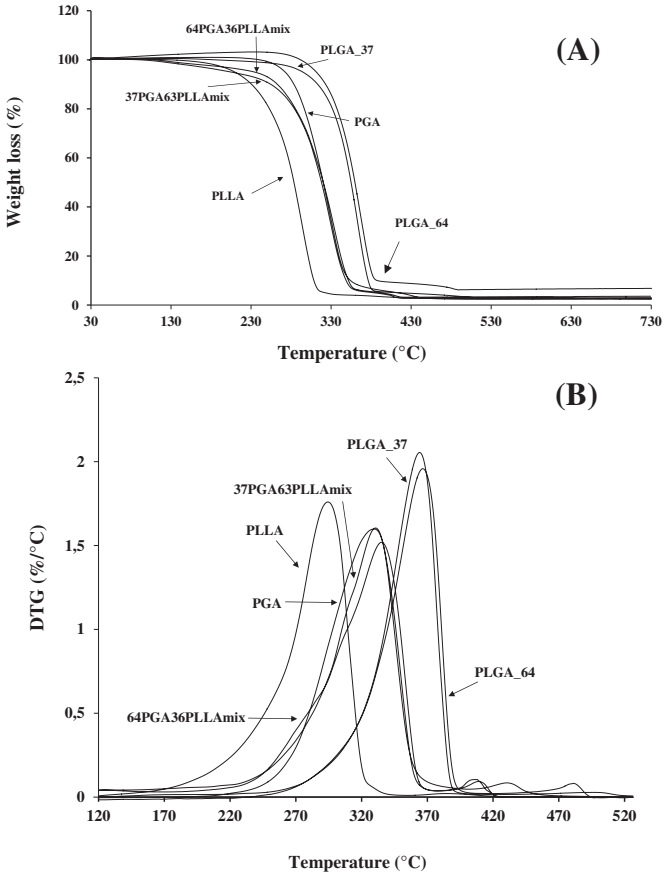

Fig. 5. TGA (A) and DTG (B) for pure polymers, copolymers, and mechanical mixtures, evaluated in air atmosphere.

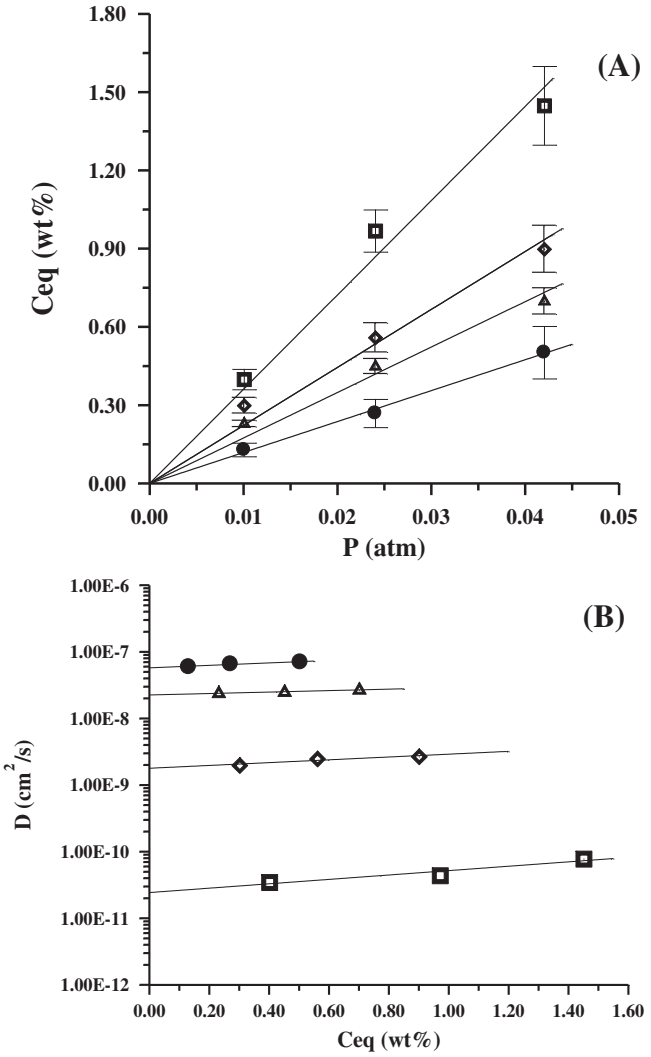

Fig. 6. C_{eq} (wt%) versus P (atm) of water vapor (A) and diffusion coefficient, D (cm^2/s), as a function of C_{eq}(wt%) of water vapor (B) for PLA (●), PLGA_37 (▲), PLGA_64 (♦), PGA (■).

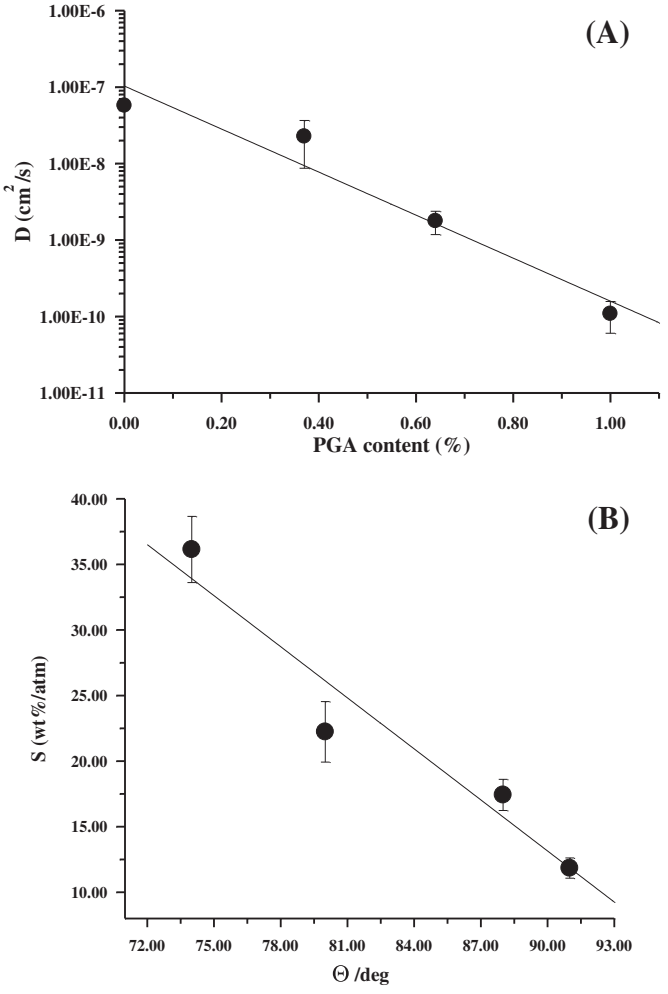

Fig. 7. (A) D_0 (cm^2/s) as a function of GA content (wt%); (B) solubility to water, S (wt%/atm), versus contact angle.

diffusion data, in terms of thermodynamic diffusion coefficient, are reported in Fig. 7(A), as a function of GA content. A linear "transformation" of the amorphous permeable phase from a "polylactic" type to a "polyglycolic" one can be observed with the GA comonomer content (Fig. 7(A)). We conducted contact angle measurements with respect to liquid water on all the samples. Fig. 7(B) shows the plot of the solubility to water, S (wt%/atm) versus contact angle. It is evident from the figure that the contact angle decreases with the increase in solubility, which is in accordance with the literature for biodegradable polyesters, whose solubility to water vapor has been correlated with the surface tension [36]. It was found that the surface tension increases with solubility. The lower the surface tension, the higher is the contact angle.

Table 3
Sorption, S (wt%/atm), thermodynamic diffusion coefficient, D_0(cm^2/s), and permeability, P (wt%/atm∗cm^2/s), to water vapor for omopolymers and copolymers.

Sample	S (wt%/atm)	D_0 (cm^2/s)	P (wt%/atm∗cm^2/s)
PLA	11.84	5.76×10^{-8}	6.81×10^{-7}
PLGA_64	17.42	2.27×10^{-8}	3.95×10^{-7}
PLGA_37	22.23	1.78×10^{-9}	3.90×10^{-8}
PGA	36.14	2.43×10^{-11}	8.78×10^{-10}

4. Concluding remarks

Biodegradable and biocompatible aliphatic poly(ester)s are generally produced by metal-catalyzed ROP of cyclic esters. An issue of concern is the removal of metal catalyst residues from the polymers. A green process for the preparation of PLGAs, PLLA, and PGA based on sodium hydride has been successfully achieved for the first time, avoiding poisonous heavy metals and in the absence of solvent. The copolymer microstructure was fully characterized by NMR. A highly randomized structure was recognized in the PLGAs by NMR and confirmed by MALDI. The mechanism of polymerization in the presence of NaH was elucidated. The presence of alcohol-functionalized end groups, observed by NMR and MALDI, supported the hypothesis of anionic ROP mechanism operating by cleavage of acyl-oxygen bond of the cyclic di-esters. Furthermore, MALDI showed the presence of carboxyl end groups, reasonably derived by the anionic initiation by cleavage of the alkyl-oxygen bond of the monomers. Both the mechanisms should be operative in the presence of NaH. Moreover, NaH can both initiate the polymerization and reduce the carbonyl groups.

Cast films were produced from all samples and analyzed. XRD analysis demonstrated that pure polymers crystallize in their usual crystalline forms, while both copolymers showed amorphous forms. The disordered chain microstructure hinders any form of crystallization. Thermal degradation analysis showed the superior characteristics of copolymers with respect to the blends. Barrier properties, sorption

diffusion and permeability of water vapor, were evaluated and correlated to the copolymer composition.

We emphasize that the experimental observations can offer valuable guidance to the design and realization of PLGAs having compositions leading to specific physical properties.

Appendix A. Supplementary data

Supplementary data to this article can be found online at http://dx.doi.org/10.1016/j.reactfunctpolym.2016.10.002.

References

[1] C. Vilela, A.F. Sousa, A.C. Fonseca, A.C. Serra, J.F. Coelho, C.S.R. Freirea, A.J.D. Silvestre, The quest for sustainable polyesters – insights into the future, Polym. Chem. 5 (2014) 3119–3141.

[2] A.C. Albertsson, I.K. Varma, Recent developments in ring opening polymerization of lactones for biomedical applications, Biomacromolecules 4 (2003) 1466–1486.

[3] O. Dechy-Cabaret, B. Martin-Vaca, D. Bourissou, Controlled ring-opening polymerization of lactide and glycolide, Chem. Rev. 194 (12) (2004) 6147–6176.

[4] A. Stjerndahl, A.F. Wistrand, A.C. Albertsson, Industrial utilization of tin-initiated resorbable polymers: synthesis on a large scale with a low amount of initiator residue, Biomacromolecules 8 (2007) 937–940.

[5] G. Gorrasi, D. Pappalardo, C. Pellecchia, Polymerization of ε-caprolactone by sodium hydride: from the synthesis of the polymer samples to their thermal, mechanical and barrier properties, React. Funct. Polym. 72 (2012) 752–756.

[6] M. Monsalve, J.M. Contreras, E. Laredo, F. López-Carrasquero, Ring-opening copolymerization of (R,S)-β-butyrolactone and ε-caprolactone using sodium hydride as initiator, React. Funct. Polym. 4 (2010) 431–441.

[7] H.R. Pohl, S.J. Wheeler, E.H. Murray, Chapter 2. Sodium and potassium in health and disease, in: A. Sigel, H. Sigel, R.K.O. Sigel (Eds.), Interrelations Between Essential Metal Ions and Human Diseases, Metal Ions in Life Sciences, 13, Springer 2013, pp. 29–47.

[8] K. Nagahama, A. Takahashi, Y. Ohya, Biodegradable polymers exhibiting temperature-responsive sol-gel transition as injectable biomedical materials, React. Funct. Polym. 73 (2013) 979–985.

[9] L. Yu, Y. Feng, Q. Li, X. Hao, W. Liu, W. Zhou, C. Shi, X. Ren, W. Zhang, PLGA/SF blend scaffolds modified with plasmid complexes for enhancing proliferation of endothelial cells, React. Funct. Polym. (2015) 19–27.

[10] I.N. Peça, K.T. Petrova, M.M. Cardoso, M.T. Barros, Preparation and characterization of polymeric nanoparticles composed of poly(DL-lactide-co-glycolide) and poly(DL-lactide-co-glycolide)-co-poly(ethylene glycol)-10%-Triblock end-capped with a galactose moiety, React. Funct. Polym. 72 (2012) 729–735.

[11] R.M. Felder, G.S. Huvard, in: R. Fava (Ed.), Methods of Experimental Physics, vol. 16, Academic Press, New York 1980, pp. 315–320.

[12] W.R. Vieth, M.A. Amini, in: Hopfenberg (Ed.), Permeability of Plastic Films and Coatings, Plenum Press, London 1974, pp. 49–61.

[13] D.K. Gilding, A.M. Reed, Biodegradable polymers for use in surgery-polyglycolic/poly(actic acid) homo- and copolymers: 1, Polymer 20 (1979) 1459–1464.

[14] L. Yu, Z. Zhang, J. Ding, Influence of LA and GA sequence in the PLGA block on the properties of thermogelling PLGA-PEG-PLGA block copolymers, Biomacromolecules 12 (4) (2011) 1290–1297.

[15] H.R. Kricheldorf, T. Mang, J.M. Jonte, Polylactones. 1. Copolymerizations of glycolide and ε-caprolactone, Macromolecules 17 (10) (1984) 2173–2181.

[16] H.R. Kricheldorf, I. Kreiser, Polylactones, 11. cationic copolymerization of glycolide with L,L-dilactide, Macromol. Chem. Phys. 188 (1987) 1861–1873.

[17] A. Meduri, T. Fuoco, M. Lamberti, C. Pellecchia, D. Pappalardo, Versatile copolymerization of glycolide and rac-lactide by dimethyl(salicylaldiminato)aluminum compounds, Macromolecules 47 (2014) 534–543.

[18] J. Kasperczyk, Microstructural analysis of poly [(L, L-lactide)-co-(glycolide)] by ^{1}H and ^{13}C NMR spectroscopy, Polymer 37 (1996) 201–203.

[19] P. Dobrzynski, J. Kasperczyk, H. Janeczek, M. Bero, Synthesis of biodegradable copolymers with the use of low toxic zirconium compounds. 1. Copolymerization of glycolide with L-lactide initiated by $Zr(Acac)_4$, Macromolecules 34 (2001) 5090–5098.

[20] J. Kratsch, M. Kurzdrowska, M. Schmid, N. Kazeminejad, C. Kaub, P. Oña-Burgos, S.M. Guillaume, P.W. Roesky, Chiral rare earth borohydride complexes supported by amidinate ligands: synthesis, structure, and catalytic activity in the ring-opening polymerization of rac-lactide, Organometallics 32 (2013) 1230–1238.

[21] M. Yamashita, Y. Takemoto, E. Ihara, H. Yasuda, Organolanthanide-initiated living polymerizations of ε-caprolactone, δ-valerolactone, and β-propiolactone, Macromolecules 29 (1996) 1798–1806.

[22] M. Visseaux, F. Bonnet, Borohydride complexes of rare earths, and their applications in various organic transformations, Coord. Chem. Rev. 255 (2011) 374–420.

[23] P. Rizzarelli, S. Carroccio, Modern mass spectrometry in the characterization and degradation of biodegradable polymers, Anal. Chim. Acta 808 (2014) 18–43.

[24] G. Montaudo, M.S. Montaudo, F. Samperi, in: G. Montaudo, R. Lattimer (Eds.), Mass Spectrometry of Polymers, CRC Press LLC 2002, pp. 428–530.

[25] M. Cocca, M.L. Di Lorenzo, M. Malinconico, V. Frezza, Crystal polymorphism of poly(L-lactic acid), Eur. Polym. J. 47 (2011) 1073–1080.

[26] C. Marega, A. Marigo, R. Zannetti, G. Paganetto, A structural investigation on poly(glycolic acid), Eur. Polym. J. 28 (1992) 1485–1486.

[27] M. Penco, L. Sartore, F. Bignotti, S. D'Antone, L.D. Landro, Thermal properties of a new class of block copolymers based on segments of poly (D, L-lactic-glycolic acid) and poly (ε-caprolactone), Eur. Polym. J. 36 (2000) 901–908.

[28] I.C. Mc Neill, H.A. Leiper, Degradation studies of some polyesters and polycarbonates: 3-polyglycollide, Polym. Degrad. Stab. 12 (1985) 373.

[29] S. D'Antone, F. Bignotti, L. Sartore, A. D'Amore, G. Spagnoli, M. Penco, Thermogravimetric investigation of two classes of block copolymers based on poly (lactic-glycolic acid) and poly (ε-caprolactone) or poly (ethylene glycol), Polym. Degrad. Stab. 74 (2001) 119–124.

[30] K. Jamshidi, S.H. Hyun, Y. Ikada, Thermal characterization of polylactides, Polymer 29 (1998) 2229–2234.

[31] A. Södergård, J.H. Näsman, Stabilization of poly (L-lactide) in the melt, Polym. Degrad. Stab. 46 (1994) 25–30.

[32] D.M. Cam, M. Marucci, Influence of residual monomers and metals on poly (L-lactide) thermal stability, Polymer 38 (8) (1997) 1879–1884.

[33] G. Gorrasi, R. Pantani, Effect of PLA grades and morphologies on hydrolytic degradation at composting temperature: assessment of structural modification and kinetic parameters, Polym. Degrad. Stab. 98 (2013) 963–971.

[34] W. Brostow, R. Chiu, I.M. Kalogeras, A. Vassilikou-Dova, Prediction of glass transition temperatures: binary blends and copolymers, Mater. Lett. 62 (2008) 3152–3155.

[35] G.L. Siparsky, K.J. Voorhees, J.R. Dorgan, K. Schilling, Water transport in polylactic acid (PLA), PLA/polycaprolactone copolymers, and PLA polyethylene glycol blends, J. Environ. Polymer. Degrad. 5 (3) (1997) 125–136.

[36] J.-S. Yoon, H.-W. Jung, M.-N. Kim, E.-S. Park, Diffusion coefficient and equilibrium solubility of water molecules in biodegradable polymers, J. Appl. Polym. Sci. 77 (2000) 1716–1722.

[37] G. Gorrasi, R. Anastasio, L. Bassi, R. Pantani, Barrier properties of PLA to water vapour: effect of temperature and morphology, Macromol. Res. 21 (2013) 1110–1117.